CHAPTER

9

Lab-on-a-Chip Impedance Detection of Microbial and Cellular Activity

Liju Yang,[1] Xuanhong Cheng,[2] Yi-Shao Liu,[3] and Rashid Bashir[3]

[1]Biomanufacturing Research Institute and Technology Enterprise, Department of Pharmaceutical Sciences, North Carolina Central University, Durham, NC 27707
[2]Department of Materials Science and Engineering, Program of Bioengineering, Lehigh University, Bethlehem, PA 18015
[3]Department of Electrical and Computer Engineering, Department of Bioengineering, Micro and Nanotechnology Laboratory, University of Illinois, Urbana-Champaign, Urbana, IL 61801

Abstract

Lab-on-a-chip type of devices capable of impedance sensing has recently attracted a lot of interest for label-free, real-time, and noninvasive electrical detection of biological activities. In this chapter, we describe four lab-on-a-chip systems for the detection of microbial and cellular activities based on the unique electrical and electrophysiological properties of micro-organisms and mammalian cells. Two of the systems were designed based on impedance monitoring of live micro-organism activities for: (1) monitoring the concentration of bacterial cells during growth, and (2) the detection of *Bacillus anthracis* spore germination. The other two systems were designed for detection of cell concentration by measuring the impedance changes due to their ion release for applications in counting: (1) CD4+ T lymphocytes, and (2) food-borne pathogenic bacterial cells. These microfabricated impedance sensors show great promise in the detection of cells and their metabolic activities with improved simplicity, higher sensitivity, and faster detection time than conventional methods.

Key terms

microfluidic chips
lab-on-a-chip
electrical detection
impedance spectroscopy
dielectrophoresis
bacteria cells
mammalian cells
cell counting
spore germination

9.1 Introduction

The advances in microelectromechanical systems (MEMS) technology have allowed scientists to construct novel devices or systems with sizes comparable to biological entities and sensitivity high enough for a wide variety of important biomedical and biological applications. Development of "lab-on-a-chip" types of devices uses MEMS technology to integrate various microfabricated sensors or detection platforms with many of the unit operations associated with sample preparation and presentation, such as separation, mixing, incubation, and concentration. The use of lab-on-a-chip devices for microbial and cellular detection has shown the following advantages over traditional methods: (1) reduction of the sensor elements to the size of a single cell or even smaller, providing a higher sensitivity; (2) reduction of reagent volume and associated cost; (3) reduction of the time to results due to the small volume and high effective concentration; (4) amenability to system miniaturization and portability; and (5) compatibility with large numbers of assays and multiplexed measurements.

Impedance sensing, as one of the principal electrical/electrochemical transductions, is becoming a fertile area for developing methods for a wide range of biological and biomedical applications. Several factors attribute to the popularity of impedance sensing: (1) the distinct electrical properties associated with specific biological entities and/or biological reactions motivate the use of impedance-sensing techniques; (2) impedance measurement is one of the most promising techniques for label-free, real-time, and noninvasive biological detection; and (3) impedance detectors can be easily miniaturized to meet the growing needs of portable systems with an analytical footprint considerably smaller than laboratory-based instruments [1].

The distinct electrical properties of biological cells and their electrophysiology are fundamental for developing impedance-based methods to detect biological activities. Biological cells consist of adjacent structures of materials that have very different electrical properties. The cell membrane consists of a lipid bilayer, where the lipid molecules are oriented with their polar groups facing outwards into the aqueous environment and their hydrophobic hydrocarbon chains pointing inwards to form the membrane interior. The inside of a cell is complex and contains membrane-covered particulates, such as mitochondria, vacuoles, a nucleus, and many charged molecules. While the cell membrane is highly insulating, the interior of the cell is highly conductive. The conductivity of the cell membrane is around 10^{-7} S/m, whereas the conductivity of the interior of a cell can be as high as 1 S/m [2].

Based on the electrophysiological and electrical properties of biological cells, three major mechanisms have been explored for the detection and quantification of biological cells using microscale impedance-based measurements:

1. *Making use of the metabolic activity of biological cells:* This is represented by impedance microbiology, which is a technique based on the measurements of the electric impedance change in a medium or a reactant solution resulting from cell metabolism [3, 4]. Based on this principle, a new technique called "impedance microbiology-on-a-chip" has been demonstrated by our group [5]. The idea is to confine a few live bacterial cells into a small volume on the order of nano- to picoliters such that metabolites of these cells are concentrated and detectable by impedance measurement with interdigitated microelectrodes. We have also

successfully developed a microchip for impedance monitoring of spore germination [6].

2. *Making use of the highly ionic cytoplasmic content of the cells:* As the inside of a cell contains many charged molecules and is highly conductive (1 S/m), the impedance change due to the lysis of cells or release of intracellular ions can provide a means to detect biological cells. In this chapter, we will review two microchip-based impedance-detection systems for: (1) enumeration of CD4+ T lymphocytes through cell lysates [7], and (2) detection of bacterial cells based on impedance change from their ion release into deionized (DI) water [1].
3. *Making use of the insulating properties of the cell membrane:* Because of their highly insulating cell membrane, cells attached on an electrode surface effectively reduce the conducting area and hence increase the interfacial impedance. The sensor probes the attachment of cells by measuring the change of the interfacial electrical properties arising from the insulating property of the cell membrane. Many cell-based impedance sensors are based on this mechanism. By culturing cells on microelectrodes and monitoring impedance changes caused by adherent cells, one can quantify changes in the impedance associated with the cell membrane, cell-substrate interaction, and cell-cell separation with exquisite sensitivity and in a noninvasive manner [8, 9]. We constructed a bacterial immunosensor based on this mechanism: antibodies specific to the target bacterial cells are immobilized on an electrode surface, and selective attachment of cells is detected electrically [10].

In this chapter, we describe four impedance-detection systems based on the first two mechanisms described above for monitoring biological metabolic activity and detecting cells.

9.2 Lab-on-a-Chip for Monitoring Microbial Metabolic Activity

9.2.1 "Impedance microbiology-on-a-chip" for bacterial concentration and detection

One common impedance method for detection of bacterial growth is *impedance microbiology*, which is based on the measurement of changes in electrical impedance of a culture medium or a reaction solution resulting from the bacterial growth. This growth-based impedance technique allows one to distinguish between viable and dead cells and to detect viable bacteria within 24 hours. In 1992, the impedance method was approved by the Association of Official Analytical Chemists International (AOAC) as the first action method for screening *Salmonella* in food samples [11, 12].

In impedance microbiology, the impedance change is typically measured using a pair of electrodes submerged in the growth medium or the reactant solution. The impedance change in the medium is mainly produced by the release of ionic metabolites from live cells. There are two main origins of ion release by bacteria into their growth environment [13]: one is energy metabolism (catabolism) in which bacteria consumes oxygen and sugars and produces carbon dioxide and organic acids; the other is ion exchange through the cell membrane. Ions (such as K^+ and Na^+) are actively transported across ion channels embedded in the cell membrane, which serves to regulate the membrane

potential and the osmotic difference between the interior and exterior of the cell. Between the two origins, energy metabolism is the major path of ion release from cells to the environment, and the ion-exchange process is a small contributor. These released ions cause changes in the ionic composition of the medium and consequently increase the conductivity of the medium. To detect bacteria, the impedance sensor measures the relative or absolute changes in conductance, capacitance, or impedance at regular time intervals during the growth of bacteria at a given temperature. The measured electrical signals are then graphically plotted on the ordinate against the incubation times on the abscissa, producing impedance growth curves. The time at which the decrease in impedance value exceeds a threshold is defined as the detection time, t_d. Generally, the impedance threshold is not reached until the bacteria number reaches approximately 10^6 to 10^7 cfu/mL (as determined by the plating method). For conventional impedance-microbiological methods, the detection time ranges from about 1 to 8 hours for initial bacterial concentration of 10^7 to 10^1 cfu/mL.

Miniaturization of an impedance-detection system into a chip-based device has shown great promise in rapid detection of bacterial growth. Our group was among the first to fabricate integrated silicon-based biochips for impedance detection of microbial metabolism [5, 14, 15]. The basic idea was to confine a few live bacterial cells into a small volume on the order of nano- to picoliters, such that the metabolites of a few live cells in a low-conductivity buffer can be rapidly detected by impedance measurements using interdigitated microelectrodes. To concentrate bacterial cells from a diluted sample into a small volume, we used a technique called dielectrophoresis (DEP), which is the electrokinetic motion of dielectrically polarized particles in nonuniform electric fields [16]. As most biological cells behave as dielectric particles in an external electric field, DEP allows trapping, concentration, and separation of biological cells in a liquid suspension.

9.2.1.1 Methods and devices

9.2.1.1.1 Chip design and fabrication

The impedance microbiology-on-a-chip device contained three sets of interdigitated microelectrodes and flow channels. Figure 9.1(a) shows the principle of the operation of the DEP-based deviation and capture of bacterial cells in the microchip. One set was for dielectrophoretical deviation of bacterial cells from the main channel into the small channel that leads to the detection chamber. In the detection chamber, one set of electrodes was for DEP capture of bacterial cell into the detection chamber, and the other set of electrodes was for monitoring the impedance change of bacterial growth in the chamber. The detection chamber had a volume of 400 pL. Figure 9.1(b) shows the cross section of the detection chamber with DEP electrodes and impedance-measurement electrodes. Figure 9.1(c) shows the completely packaged microchip.

The microchips were fabricated on 4" wafers with a (100) surface and a thickness of 500 μm. Electrodes and channel patterns were made using standard photolithographic technology. The channels were 12 μm deep and were made by etching the wafer with a hard mask. The DEP electrodes were deposited by sputtering 1,000Å of aluminum onto 2,000Å of silicon dioxide on the bottom of the channel. On the DEP electrodes, another layer of silicon dioxide of 3,500Å was deposited by plasma-enhanced chemical vapor deposition in order to completely isolate the DEP electrodes and prevent electrolysis of the liquid in the channels. The impedance-measurement electrodes and temperature

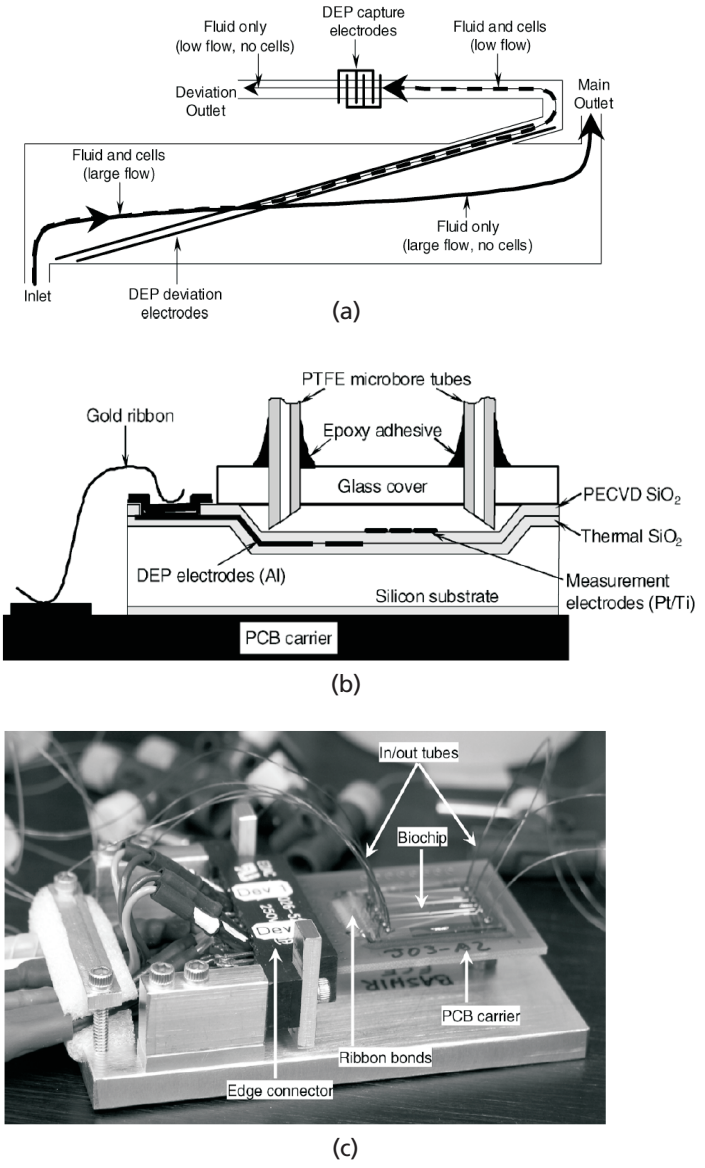

Figure 9.1 (a) The schematic design of the microchip with DEP deviation electrodes in the main channel and a small channel leading the flow to the DEP capture electrodes in the detection chamber. (b) Simplified cross section of the packaged microchip showing the DEP capture electrodes and the impedance-measurement electrodes in the detection chamber. (c) An image of the packaged microchip connected to the measurement and control system. (Reprinted with permission from the *J. Microelectromechanical Systems* and kind permission from [5].)

sensor were deposited by sputtering 800Å of platinum over a titanium adhesion layer. The chip was assembled with a glass cover with inlet and outlet holes using anodic bonding. Detailed procedure can be found in [5].

9.2.1.1.2 Bacterial cell preparation

Listeria monocytogenes v7 was grown in Luria-Bertani (LB) medium at 37°C for at least 16 hours. The cells were harvested and washed by repeated centrifugation and resuspension in sterile LB medium. The cells were then diluted in sterile LB to desired concentrations. When fluorescent cell were needed, 1 mL of the as-grown live cells was stained with green fluorescent dye $DiOC_6(3)$ (3,3′-dihexyloxacarbonanine iodide). Fluorescence-stained cells were washed and diluted in the same way as described above for further use.

9.2.1.1.3 On-chip DEP concentration and impedance detection of metabolism

All the on-chip experiments were carried out with the chip heated to 37°C. A total volume of 40 μL of the cell suspension in DI water was injected into the main channel at a flow rate of approximately 1.7 μL/min. The DEP deviation and capture electrodes were excited with a 16 V_{pp} square signal at 100 kHz. During the injection, the flow rate in the incubation chamber was manually controlled to be between 4 and 10 nL/min. After the sample injection, the DEP deviation electrodes were turned off, and Half-LB medium (HLB, mixing equal parts of LB and DI water) was injected at a flow rate of less than 0.5 μL/min, while the excitation voltage on the capture electrodes was increased to 20 V_{pp}, and the frequency was increased to 3 MHz in order to maximize the DEP forces acting on cells. Once the incubation chamber was filled with HLB, the flow was stopped, and the fluidic channels and microtubes were pinched to seal them completely. The DEP capture electrodes were then turned off. Impedance measurement electrodes were turned on, and the cells were incubated for approximately 12 hours. The impedance was measured with an Agilent 4284A LCR meter (Agilent Technologies Inc., Palo Alto, California) connected to the chip through an Agilent 34970A switching unit fitted with two Agilent 34905A RF multiplexer cards. All the instruments were connected to a computer through a GPIB interface. The impedance measurements and chip temperature were controlled by custom LabVIEW program (National Instruments Corp., Austin, Texas). Impedance was measured at 51 frequencies logarithmically spaced between 100 Hz and 100 kHz, with a 150 mV amplitude. Sinusoidal and square wave DEP signals were generated by Agilent 333120A synthetized signal generators.

9.2.1.2 Results and discussion

To demonstrate the complete process of cell concentration and impedance measurement of bacterial metabolism on the chip, samples containing fluorescently labeled *L. monocytogenes v7* cells at concentrations of 2.3×10^5, 6.8×10^5, and 8.7×10^4 cfu/mL were tested. The sample with 2.3×10^5 cfu/mL cells was injected with the DEP electrodes off, while the other two samples were injected with the DEP electrode activated. When the DEP electrode was off, the cells were not concentrated in the incubation chamber. There was only a probability of approximately 0.09 to find one cell in the chamber. When DEP electrodes were activated, almost all the cells were captured by the DEP electrodes into the detection chamber. Figure 9.2(a) shows a representative image of fluorescently labeled *Listeria* cells concentrated by DEP into the picoliter measurement chamber. Although the actual number of cells collected was not determined, it was visually confirmed that only a very small fraction of cells escaped the DEP deviation and capture processes (no more than approximately 10%). However, during the switch from water to HLB, a more significant fraction of the cells were lost because the DEP

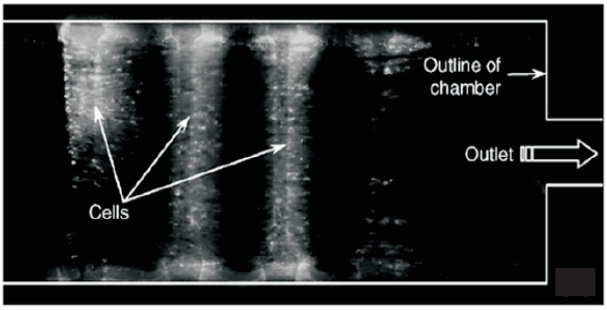

(a)

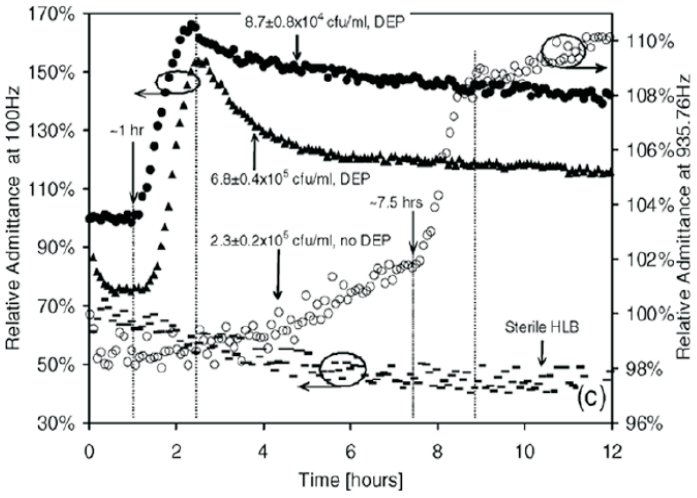

(b)

Figure 9.2 (a) Fluorescence-labeled *Listeria* cells concentrated by DEP from a suspension of 6.8×10^5 cfu/mL into the incubation chamber immediately before the start of incubation. (b) Relative admittance change during the incubation of *Listeria* cells injected into the microchip at various concentrations, with and without DEP concentration, plus sterile HLB. Values at $t = 0$ are defined as 100%. (Reprinted with permission from the *J. Microelectromechanical Systems* and kind permission from [5].)

force was weakened by the increased medium conductivity and the fluctuation of the flow rate. Nonetheless, thousands of cells were still collected in the chamber, as shown in Figure 9.2(a). The concentration factor of this chip was between 10^4 to 10^5 when the cells in an original sample volume of 40 μL were concentrated into the 400 pL chamber, provided that 10% to 100% of the cells were captured by DEP. Such DEP concentration technique in microfabricated chips eliminates the need to enrich the bacterial population by long culture steps in conventional cell culture methods. With the dramatic increase of bacterial cell concentration at the locality of the detection chamber, it is expected that the detection time on the impedance growth curve can be effectively reduced, resulting in rapid detection.

The significant reduction in detection time was demonstrated by the comparison of the impedance growth curves of *Listeria* cells in HLB medium on chip with and without DEP concentration [Figure 9.2(b)]. As shown in the figure, the sterile media did not exhibit any clear metabolic signal at any frequency. The bacterial sample containing approximately 6.8×10^5 cfu/mL with the DEP concentration presented an impedance

metabolic signal corresponding to the exponential growth at approximately 1 hour, while the sample containing similar concentration of cells without DEP concentration required approximately 7.5 hours to produce a detectable impedance signal. The results demonstrated that concentration of bacterial cells by the DEP can effectively shorten the detection time needed for the impedance detection of cell metabolic activity.

Miniaturized sensors for impedance-based detection of bacteria integrated with a DEP-based cell-concentration system hold great potential to dramatically reduce the time needed to detect bacteria based on their metabolic activity to hours, which is a great improvement compared with conventional methods that require several days. Such a microscale system also has great potential applications for screening industrial and clinical samples for total bacterial contents.

9.2.2 Microfluidic biochips for impedance detection of *Bacillus anthracis* spore germination

Bacillus anthracis has long been identified as the causative agent of the disease anthrax. The intentional contamination of seven letters with *B. anthracis* spores in 2001 resulted in 22 cases of anthrax, 5 of which were fatal [17], and focused attention on the detection of spores of *Bacillus anthracis*. *Bacillus anthracis* has a long-term environmental persistence due to the formation of endospores, which develop over a time course of several hours inside a cell exposed to nutrient starvation or other environmental stresses [18]. A dense protein coat, low cytoplasmal water activity, and small, acid-soluble, DNA-binding proteins render the spore highly resistant to dessication, irradiation, chemical oxidation, and other environmental assaults [19]. This resistance renders decontamination of an environment in which endospores are present very difficult and makes detection of low-level spore contamination an important goal. Many detection methods, such as colony morphology, staining of the unique poly-D-glutamate capsule, PCR amplification of specific DNA sequences, and c-phage susceptibility testing, require the outgrowth of vegetative cells before testing; they also often require time-consuming manual steps. Several innovative methods reported in recent years can detect endospores at a threshold of about 10^3 spores in a sample [20–25]. Most of these methods involve micro- or macroscale PCR analysis or various forms of optical detection. Automated spore-detection systems have used real-time PCR with thermal cycling chambers made from etched and fusion-bonded silicon to carry out the PCR-based detection assays for *Bacillus* spp. and *Yersinia* spp. [26]. It should be noted that most of the reported methods either perform identification of the spores before spores germinate and fail to distinguish between viable and nonviable spores [21], or they detect the pathogens at relatively late vegetative growth phase [20]. In this section, we review a detection method for viable spores by impedance measurement. The detection was performed as early as the spore-germination stage, and a signal was detected only when the spores were viable.

9.2.2.1 Methods and devices

We first examined the concept using macroscale experiments, where we measured the germination of a 5 mL spore suspension, with concentration ranging from 10^7 to 10^9 spores/mL, in a rinsed (with sterile DI water) and sterile 15 mL plastic centrifuge tube (430052, Corning Inc., Corning, New York) using a commercial conductivity meter

(6307 microcomputer pH/conductivity meter, Jenco Instruments, San Diego, California). The spores were preheated in a 65°C water bath for 30 minutes before the experiment. Afterwards, germinant solution was added, and the conductivity probe was inserted into the 15 mL centrifuge tube containing the sample. Conductivity values were recorded every minute. Three different concentrations of spores were compared to control experiments (i.e., spores only, DI water only, and germinant only) to find the detection limit. The conductivity probes were calibrated before each experiment. The DI water had a measured conductivity of 2 to 3 μS/cm, which was within the accepted range and thus demonstrated the sensitivity of the instrument. The experiment was carried out at room temperature [27].

The microfluidic device for on-chip detection of spore germination was constructed as a three layer BioMEMS device. The first layer was a Pyrex (7740, Corning Inc.) substrate with interdigitated electrodes for exerting dielectrophoresis force to capture and concentrate spores and for recording the change of admittance (inverse of impedance) within the solution. The metal electrodes were deposited as 250Å titanium and 350Å gold by evaporation (E-Beam Evaporator, CHA Industries, Fremont, California), followed by a lift-off process. On top of the Pyrex substrate was a 40 μm PDMS layer with patterned microfluidic channels and chambers for sample delivery and germination detection. The third layer was a thick, 2 mm PDMS slab with microfluidic pathways serving as valves to close off the channels in the thin second layer to enhance the signal strength by forming a closed environment for detection, as well as to constrain spores inside the detection chamber after the dielectrophoresis (DEP) capture force was released. The layout of the chip and the completed chip are illustrated in Figure 9.3(a, b). The Pyrex layer containing the electrode substrate and the hybrid PDMS layer was bonded by surface treatment using oxygen plasma (200W, 15 seconds) and aligned immediately (within 5 minutes). The etch gas was 80% argon and 20% oxygen. Microbore tubings (OD: 0.016", ID: 0.006", Cole Parmer, Vernon Hills, Illinois) were inserted into the punched inlet holes and sealed with 10:1 PDMS for injection of liquids. The cross section of the fabricated biochip and its functions is illustrated in Figure 9.3(c) [28–30].

The electrical measurements on-chip were carried out with an automated recording system. The system included an injector, measuring probes (Micromanipulator Co., Carson, Nevada), an LCR meter (Agilent Technologies), a computer, and a microscope (Eclipse E600FN, Nikon Inc., Melville, New York). Heat-treated spores were injected by the injection system into the microfluidic device mounted on the microscope platform, with a flow rate of 30 μL/min for 5 minutes, followed by 0.2 μL/min. The injection system had multiple injection valves and switches to change solutions for delivery of samples and germinant. Electrical recording started right after spores and germinant were delivered into the chip. Data was recorded at 2-minute intervals for 1 hour. Verification of germination after each experiment was done by observing the refractility of *Bacillus anthracis* spores using phase-contrast microscopy. Ungerminated spores are refractile (phase bright) and germinated spores are not (phase gray or phase dark). The experiment was carried out at room temperature.

9.2.2.2 Results and discussion

The results of spore-germination detection with a commercial conductivity meter are illustrated in Figure 9.4(a). This figure shows the results with spore concentrations of

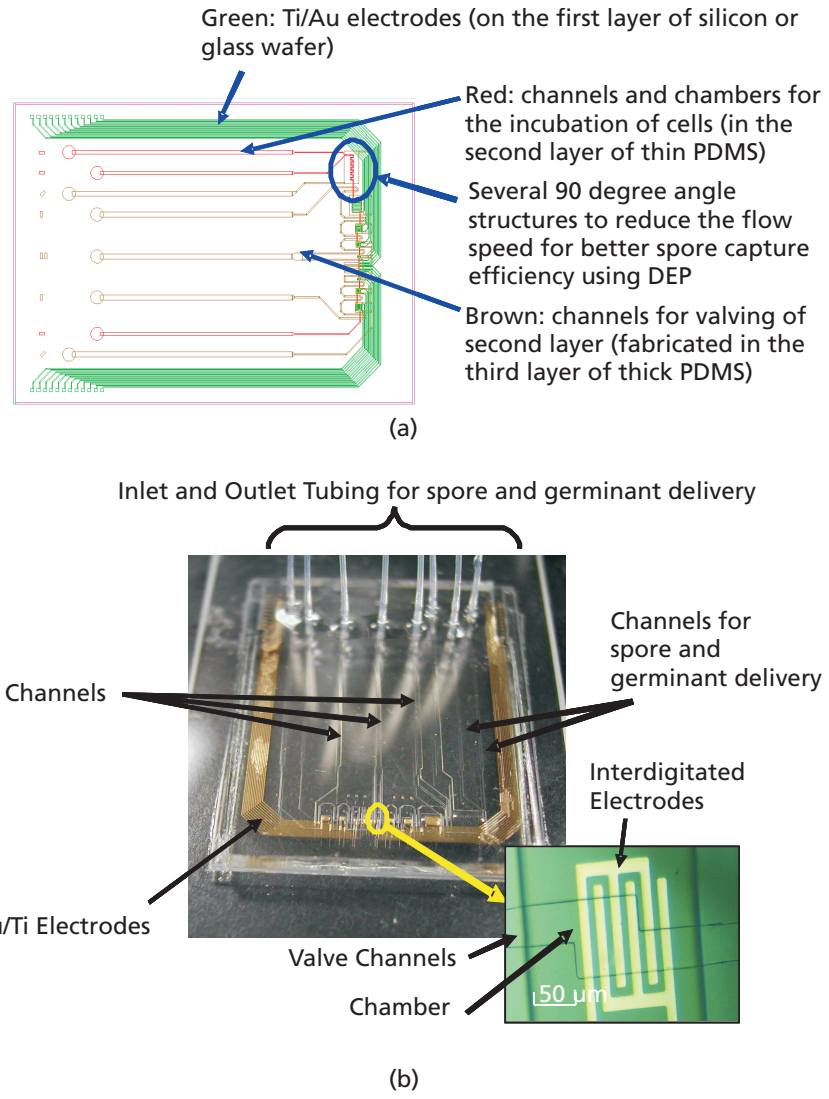

Figure 9.3 (a) Top-view layout of the microfluidic device, (b) optical image of the completed device, and (c) cross section of the microfluidic device. Spores were heat-activated off-chip, then passed through and captured on interdigitated electrodes by DEP in the desired chamber. (d) Valving is effected by pressurizing the third layer and thus pressing against the second layer channel to form a closed environment for spore germination to take place. The effectiveness of the valves was demonstrated with a solution of safranin dye. (e) Fluorescence microscope image of spores captured within the chamber using DEP forces. 20V peak-to-peak, 100 kHz. Total elapsed time is 1 minute. Activated spores stained with the FITC dye, $DiOC_6(3)$. (Reprinted with permission from *Lab on a Chip* and kind permission from [6].)

10^7, 10^8, and 10^9 spores/mL. The most pronounced result is observed at a concentration of 10^9 spores/mL, where a net increase of conductivity occurs in the range of 5 to 7 μS/cm. An immediate increase in conductivity suggests that germination began in the first 2 minutes after germinant was added and finished within 20 minutes, while control experiments showed no significant change in conductivity over time. We consid-

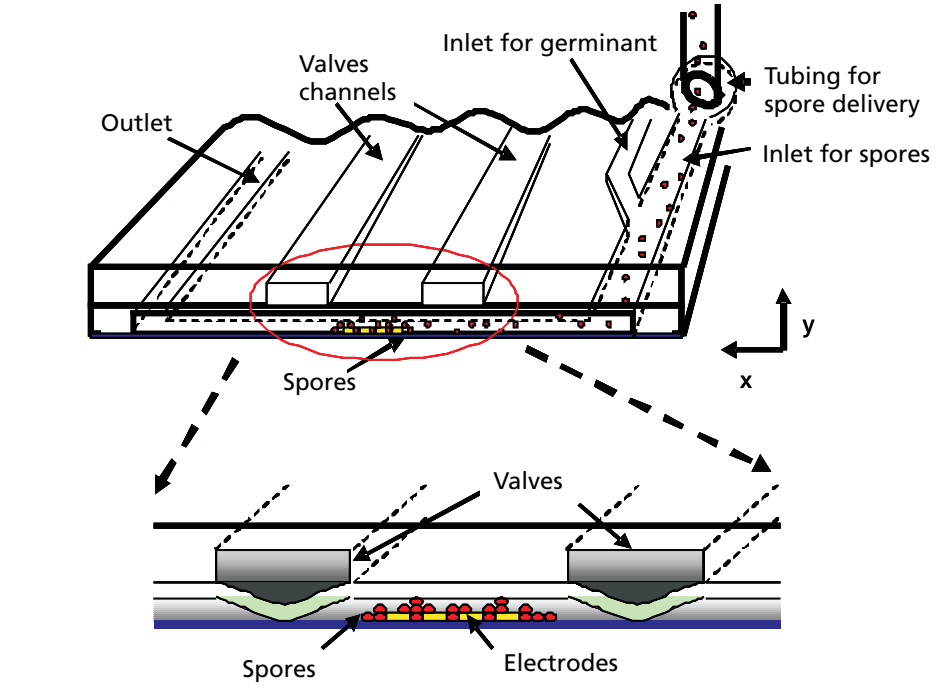

(c)

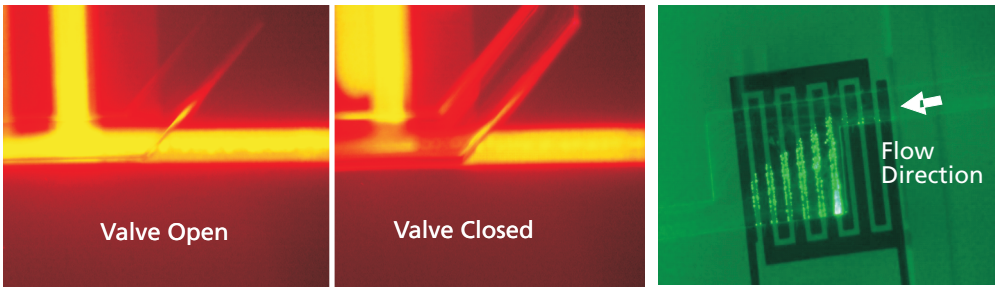

(d) (e)

Figure 9.3 (continued)

ered the 10^9 spores/mL concentration as the one that can be safely detected and used this value for the design of the microscale assay.

In microfluidic device experiments, spores were delivered to the target chamber (0.1 nL, $100 \times 100 \times 10\ \mu$m) in a carrier stream of DI water. The spores were captured at the edge of the embedded electrodes by dielectrophoretic forces induced at 20V and 100 kHz. With a flow rate of 0.2 μL/min (peak flow velocity: 40 cm/min), 90% of the spores in the carrier stream were captured by DEP [31]. Figure 9.3(e) shows the capture of spores by DEP forces, 20V peak to peak, 100 kHz.

We first germinated the spores without actuating the built-in valves. Measurement of admittance started right after the germinant solution had fully replaced the DI water.

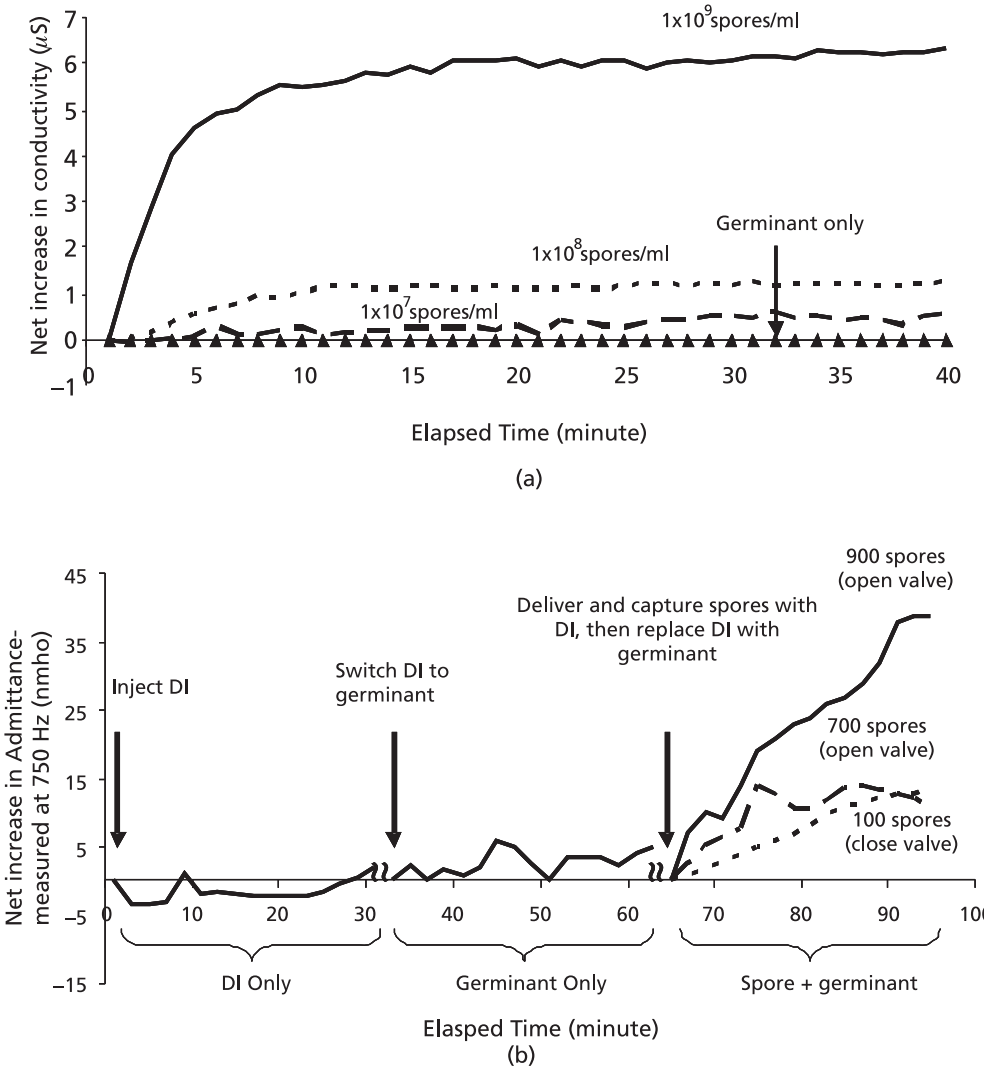

Figure 9.4 (a) Impedance curves of the spore germination in the macroscale germination experiments with samples containing 10^9, 10^8, and 10^7 spores/mL. The control sample contains germinant solution only. (b) Representative on-chip experimental results with about 100, 700, and 900 spores in a 0.1 nL chamber (graphs of data with 700 and 900 spores were open-valve experiments, while the graph with 100 spores was from a closed-valve experiment). The results from serially performed control experiments are also shown. (Reprinted with permission from *Lab on a Chip* and kind permission from [6].)

The results showed an increase in admittance upon spore germination [Figure 9.4(b)]. In comparison to the control experiment with germinant only, the samples with approximately 700 spores and approximately 900 spores presented significant increases in admittance, starting 2 minutes after the experiment began. There was no significant increase in admittance in the control experiments. Fluctuations in admittance occurred because the chamber was open to the flow stream without the actuated valve. However, when spores started to germinate, enough ions were released to overcome the baseline fluctuation and showed a significant increase in admittance. The detection limit with this experiment proved to be a few hundred spores in a 0.1 nL chamber.

To overcome the problem of fluctuations in admittance, the designed microfluidic valves were actuated to isolate the germination chamber from the rest of the system. The channels in the third layer of the microfluidic device (the PDMS slab) were pressurized with germinant solution to close the valves in the second layer [the PDMS membrane; see Figure 9.3(c, d)]. We used germinant solution to close the valves in order to avoid admittance perturbation due to ion permeation from the valve channel into the germination chamber through the PDMS layer. Two sets of sensing probes were used to measure two identical chambers (0.1 nL) simultaneously, with one serving as a control chamber and the other as the experimental chamber. A comparison of the results from these two identical chambers determined that the chamber with spores and germinant had a significant increase in admittance when germination was taking place, whereas the control chamber showed no significant difference from the control experiments without germinant. The sample with 100 spores showed an immediate increase in admittance and reached an admittance increase of approximately 10 nmho in 20 minutes. It is clear that only when spore germination was taking place did a significant change in the measured signal occur. (There was a slight admittance increase in the control chamber in the germination experiment due to the influence of ions permeating the PDMS from the experimental chamber.) Based on a comparison of the admittance changes with 700 spores in the open-valve experiment and with 100 spores in the closed-valve experiment, results were very similar, indicating that the isolation valves also enhanced the sensitivity of the admittance measurements. This implies that a lower detection limit could be achieved by including isolation valves in the chip design. The detection limit was less than 100 spores in a 0.1 nL chamber (10^9 spores/mL). Theoretically, this limit could be reduced to 10 spores or even 1 spore with smaller-sized chambers.

In this study, we demonstrated a method for automatic and rapid electrical detection of germination of viable spores within a microfluidic biochip. The microfluidic device includes special design features that facilitate spore capture and isolation as well as electrodes for spore concentration and impedance measurements. The limit of detection was shown to be a few hundred spores in a 0.1 nL chamber without use of the isolation valves. The detection limit was reduced to fewer than 100 spores in a 0.1 nL chamber when the chamber was isolated by closing the isolation valves. The detection limit can be further lowered by using a smaller capture-measurement chamber. The detection time is as short as 2 hours from heat activation of a suspected organism, which makes the impedance-based detection method a promising candidate for an on-site environmental diagnostic platform.

9.3 Lab-on-a-Chip for Impedance Detection of Cell Concentration Based on Ion Release from Cells

9.3.1 Microchips for impedance detection of CD4+ T lymphocytes

Although multiple miniaturized platforms exist for cell counting in suspension, such as flow cytometry and Coulter counters [32–35], methods to enumerate attached cells within microfluidic devices are limited. Optical-microscopy-based cell detection, although straightforward, remains dependent on a stable light path and lensing, filtering, and focusing mechanisms that add cost and complexity to detection. In addition,

optical detection tends to be low throughput due to the small detection area available at a single time. A valuable complement to optical microscopy is surface impedance sensing to enumerate cells attached on a substrate [36–38]. However, in the impedance-sensing method, a near unity of cell coverage on the electrode surface is required to generate a detectable signal.

To address the need for sensitive detection of a small number of cells attached on a relatively large surface area or in a large volume, we introduce in this chapter an approach called "cell lysate impedance spectroscopy." In this approach, surface-bound cells are lysed in a microfluidic channel, and the bulk conductance changes are measured through surface-patterned electrodes and impedance spectroscopy. As the intracellular ion content is relatively constant in each cell type, the number of released ions measured electrically is indicative of the cell number. Using immunoaffinity-isolated CD4+ T cells as an example, we demonstrate here that bulk solution conductance increases proportionally to the number of cells in the microdevice. In addition, this method has a detection threshold of 20 cells/μL, which is sufficiently useful for many clinical and research applications that require cell counting.

9.3.1.1 Methods and devices

Microfluidic devices were fabricated by bonding two pieces of glass slide with a PDMS gasket that is 50 μm thick and contains an opening window of 5 cm $\times$ 4 mm. The PDMS gaskets were prepared by curing spin-coated PDMS on a transparency slide, followed with hand-cutting windows of desired sizes. Interdigitated (IDT) gold electrodes were patterned on the bottom slide by standard photolithography [Figure 9.5(a)], facing to the microfluidic channel side during assembly. Two holes were drilled on the cover slide and bonded with PDMS ports to form fluid inlets and outlets. Assembled devices were then functionalized with a monoclonal CD4 antibody and primed with PBS containing 1% BSA and 1 mM EDTA [7]. CD4+ T lymphocytes from healthy donors were captured in the microfluidic chip by flowing cultured peripheral blood mononuclear cells (PBMC) into the device at 5 μL/min. This flow rate is optimal for efficient and specific capture of CD4+ T lymphocytes [7], and the duration of sample injection determines the total number of captured cells.

To minimize background conductance, we use the following operational sequence to lyse the captured cells: First, extracellular ions present in the microchannel were washed out using a low-conductive washing solution containing 8.5% sucrose and 0.3% dextrose at a flow rate of 20 μL/min until impedance signals were stable. This ion-free solution has been found to maintain viability of mammalian cells. Next, a low-conductive solution containing 2% sucrose and 0.07% dextrose was flowed in at a flow rate of 10 μL/min for 1 minute for controlled cell lysis. The lysing solution was formulated such that cell lysis occurred after a complete replacement of the washing solution by the lysing solution. Cells were then kept in the lysis solution in a static state for another 10 minutes to allow cell lysis to reach a steady state.

Impedance measurements were taken using an Agilent 4284 LCR meter (Agilent Technologies). The microelectrode devices were connected to the LCR meter through platinum probes. The impedance-measurement process was automated by custom LabVIEW (National Instruments Corp.) virtual instruments and GPI B interface. Imped-

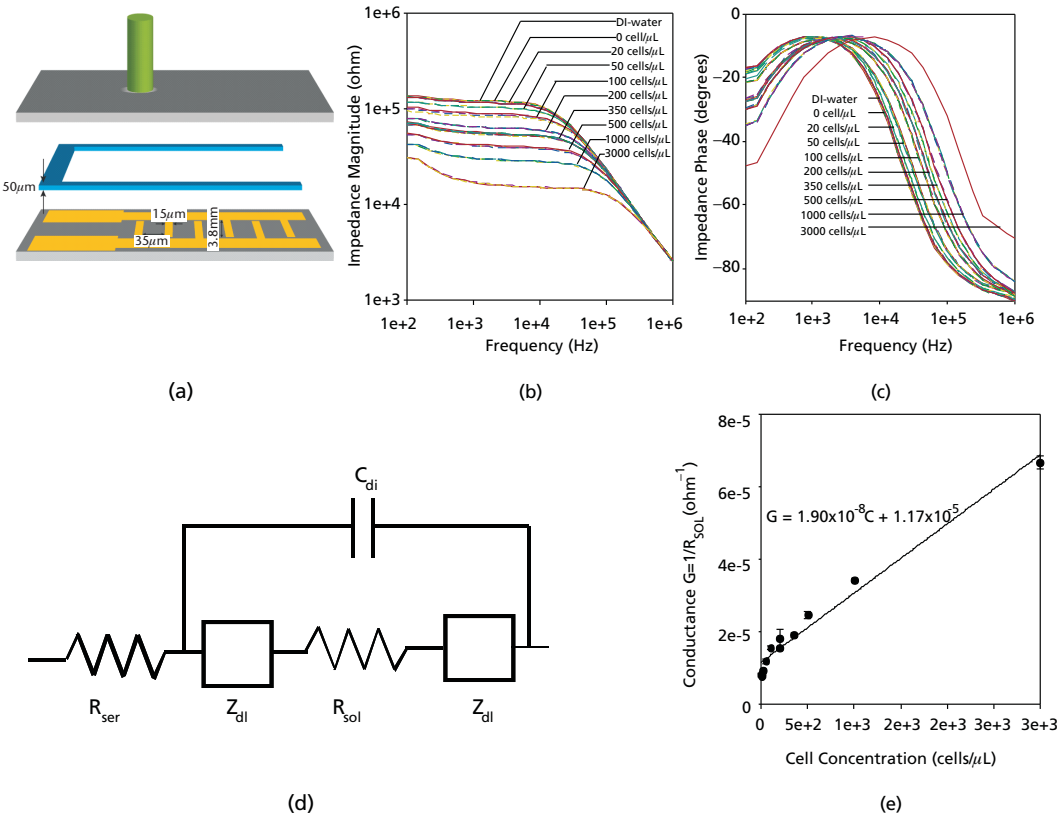

Figure 9.5 Microfluidic devices used in this study and impedance spectroscopy measurement using off-chip cell lysate. (a) The devices are composed of two glass slides with micropatterned IDT electrodes and a PDMS gasket. (b) Impedance magnitude and (c) phase spectra of DI water and cell lysate with different starting cell concentrations measured on the IDT device. Three to five scans were performed at each cell concentration in the frequency range between 100 and 10^6 Hz. (d) An equivalent circuit used in our study to model the electrode/electrolyte system for extracting bulk solution conductance, $1/R_{sol}$, which directly correlates with cell ion release [1]. (e) A linear relationship between measured bulk solution conductance (solid dots) and cell concentration is observed, and the best fits are shown as solid lines. Error bars indicate the standard deviation from three to five continuous measurements within a single device. (Reprinted with permission from *Lab on a Chip* and kind permission from [7].)

ance spectra were measured in the frequency range of 100 Hz to 1 MHz with a frequency increase factor of 1.5 and amplitude of 250 mV.

9.3.1.2 Results and discussion

To test the detection sensitivity of ions released from primary cells using impedance spectroscopy, we first lysed PBMCs of known concentrations in Eppendorf tubes with DI water and measured the impedance of the lysate using the microfluidic device with coplanar interdigitated microelectrodes (IMEs) as shown in Figure 9.5(a). Figure 9.5(b, c) shows the spectra of impedance magnitude [Figure 9.5(b)] and phase [Figure 9.5(c)] as a function of frequency for cell concentrations ranging from 0 to 3,000 cells/μL mea-

sured using the IMEs. We observed that each spectrum has two regions, a constant-impedance region in the frequency range from 100 Hz to 10 kHz and an impedance-decreasing region when frequency is greater than 100 kHz. With increasing cell concentrations, there is a consistent decrease in impedance magnitude in the low-frequency range and a shift of phase peak to higher frequency. This suggests strongly that semiquantitative measurement of cell number can be achieved through ion release.

To understand solution conductance as a function of cell number, we carried out modeling studies to extract bulk conductance from the impedance spectra. Electrodes in an electrolyte solution can be modeled using an equivalent circuit as shown in Figure 9.5(d) [5, 7], where C_{di} is the dielectric capacitance (it contains dielectric contributions from all the materials surrounding the electrodes, including the solution), R_{sol} is the bulk solution resistance (charge transport across the bulk solution), Z_{dl} is the interfacial impedance (the so-called Warburg impedance that accounts for the change in the ionic gradient at the interface), and R_{ser} is the resistance of the on-chip wiring. The interfacial impedance can be expressed as

$$Z_{dl} = 1/\left[(j\omega)n\,B\right] \tag{9.1}$$

where $j = \sqrt{(-1)}$, and n and B are parameters dependent on the properties of the electrolytes and the electrodes. This is the simplest model that would properly fit the measured data over the whole frequency range at all times. Solution bulk conductance G_{sol} is simply the reciprocal of R_{sol}.

By applying the circuit model to the group of curves in Figure 9.5(b, c), bulk conduction was extracted and plotted as a function of cell concentration [solid dot in Figure 9.5(e)]. It is observed that solution conductance increases linearly with the number of cells, confirming our hypothesis that ion release and solution conductance change are indicative of cell number. Moreover, using ion release to detect cells appears to be extremely sensitive and can detect as few as 20 cells/μL in an ion-free solution. The slope of the conductance curve represented measurement sensitivity of the microchip, and the sensitivity of the IMEs was about 1.90×10^{-8}/cell μL.

After impedance measurement using off-chip lysate, we then studied how impedance changes in the process of cell capture and on-chip cell lysis. CD4+ T cells were captured from cultured peripheral blood mononuclear cells, followed with washing with PBS buffer and then the low-conductive washing solution. Afterwards, the low-conductive cell-lysing solution was introduced into the microfluidic device, and cells were allowed to lyse for 10 minutes. At the end, the reference spectra were obtained with DI water. In the entire process, impedance spectra were acquired continuously and reflected the bulk solution resistance. Take the impedance magnitude at 760 kHz, for example [Figure 9.6(a)], where maximum separation occurs between the impedance magnitude curves in Figure 9.5(b), it remains in the low kilo-ohm range when cells are in PBS due to the high ionic concentration of biological buffers. It increases dramatically to above 10 kΩ upon introduction of the low-conductive washing solution. When cells are kept in the low-conductive washing solution in a static state, impedance magnitude decreases slightly, likely due to cell ion release in a low-conductive environment. After injection of the ion-free lysing solution, an initial impedance jump is noticed because the lysing solution has a lower conductivity than the washing solution. This is followed

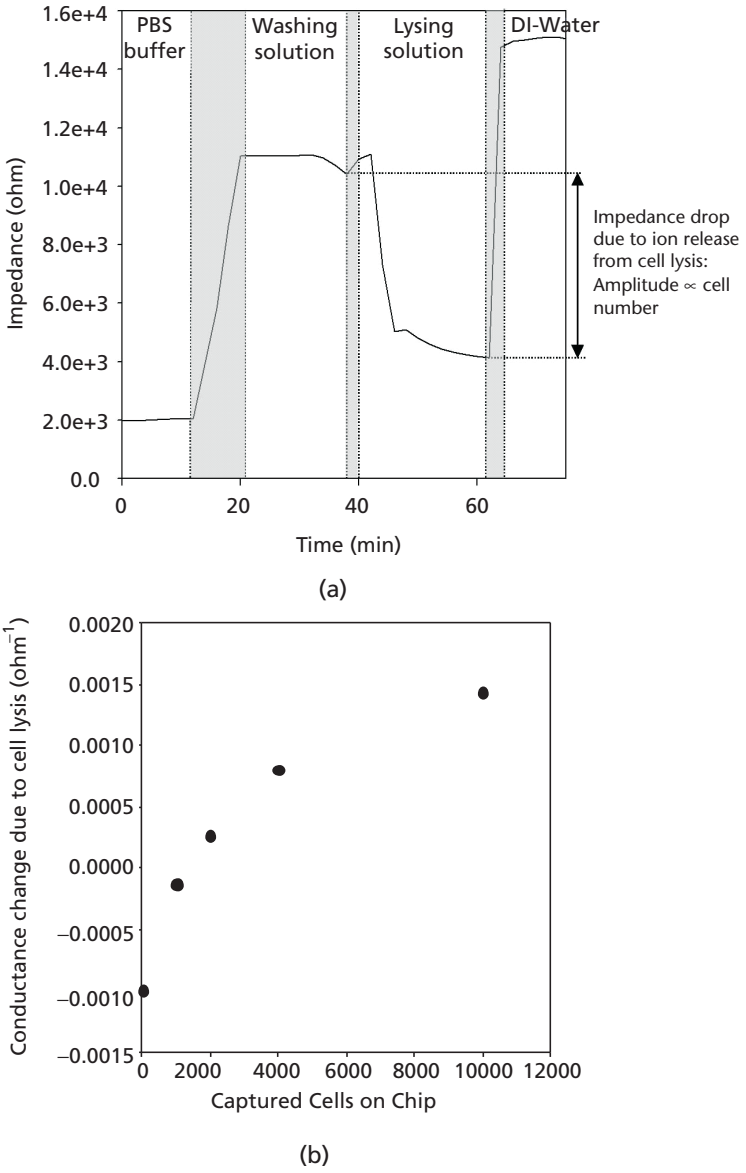

Figure 9.6 (a) Impedance measurement at 760 Hz in the process of cell capture and on-chip lysis. The respective incubation steps are labeled on top of the graph, and the shaded areas between these labeled steps are transient states during solution exchanges. The impedance drop before and 10 minutes after injecting the lysing solution is associated with cell lysis and used as a cell-numbers indicator. (b) Conductance change in the process of on-chip cell lysis versus the number of cells captured within microfluidic devices. Bulk solution conductance was extracted from the impedance spectra, and conductance drop before and 10 minutes after flowing in the lysing solution was taken as the indicator to count cell. This conductance change increases continuously with the number of cells captured within the microfluidic chip, suggesting immobilized cells can be counted by electrical measurement of their ion release. Nonlinearity of the relationship may arise from incomplete diffusion of ions within the measurement time. Each data point in the plot represents measurement from one device. (Reprinted with permission from *Lab on a Chip* and kind permission from [7].)

with an abrupt drop of impedance and a subsequent slower impedance decrease. This two-stage impedance drop during cell incubation in the lysing solution matches optical observation of lysed cell numbers in the same solution (data not shown), suggesting that the decrease in impedance magnitude arises from lysis of the captured cells.

Following the same data-fitting procedure as described above, bulk conductance was extracted from the impedance spectra and the conductance change before and 10 minutes after flowing in the lysing solution was taken as a result of complete ion release from captured cells. When we compare this conductance change to manual cell counts within the microfluidic devices [Figure 9.6(b)], it is evident that the bulk conductance change is proportional to the number of captured cells. The results successfully demonstrate that cells can be detected and counted within a microfluidic device through the impedance/conductance measurement of cell lysate.

In conclusion, impedance spectroscopy can be used to detect mammalian cells immobilized in a microfluidic device through their ion release. The microdevice helps to confine the ions in a small volume for sensitive measurement. Not only is the approach useful for terminal cell counting, but it also holds the promise to study live-cell activities through their ion exchange with the environment.

9.3.2 Interdigitated microelectrode chip for impedance detection of bacterial cells

The conductivity of bacterial suspensions has been used to study the electrical properties of bacterial cell-surface and related cell-surface interfacial physiology [39, 40]. It can also be used to quantify the concentration of bacterial cells in suspensions. We present here a simple and rapid impedance method to detect bacterial cells in suspensions using interdigitated microelectrodes.

When bacterial cells are suspended in DI water, there are two possible ways for the bacterial cells to alter the impedance of DI water. One is via the charged nature of bacterial cell surfaces. The bacterial cell walls contain various acidic groups such as carboxyl, phosphate, and amino groups [41]. Generally, there is a higher concentration of anionic groups than of cationic groups, which results in a negative cell-wall charge at neutral pH. This charge is compensated for by counterions that penetrate into the porous cell wall and, to a minor extent, by coions that are expelled from it, thereby conferring electrostatic charge to the cell periphery [39, 40, 42]. The charge density of the bacterial cell wall can be as high as 0.5 to 1.0 C/m^2 [39]. The conductivity of the DI water is in a range from as low as about 1 to 2 μS/cm to up to about 10 to 15 μS/cm. When bacterial cells are suspended in low-conductive DI water and reach a sufficient concentration, they can alter the conductivity of the suspension because of their cell-wall charges. The other way for bacterial cells to alter the conductivity of DI water is via the ion release from bacterial cells. When bacterial cells are suspended in a solution, such phenomena may occur as leakage of ions through the cytoplasmic membrane and negative adsorption of electrolyte or ion uptake into the cytoplasm and specific adsorption of ions. These processes can influence the conductivity of the bulk solution [39]. When bacterial cells are suspended in DI water, they experience an osmotic shock. In response to the fluctuations in environmental osmolarity, cells adjust their intracellular solute concentrations in order to maintain a constant turgor pressure and ensure continuation of cellular activity. Other properties of cells, such as cell size and buoyant density, can also be altered in

response to the osmotic shock [43]. The charges on the cell wall, the release of ions, and other responses to the osmotic shock in combination account for the impedance change in DI water with suspended bacteria.

Here, we used *Salmonella typhimurium*, a Gram-negative, food-borne, bacterial pathogen, as an example to demonstrate impedance detection of bacterial cells in suspensions. *Salmonella* cell suspensions in DI water and phosphate buffered saline (PBS) solution were studied over a wide range of frequencies. Bacterial cells suspended in DI water with different cell concentrations were shown to have different electrical impedance spectral responses. In a certain frequency range, impedance of the cell suspension is directly proportional to the cell concentration, which can be used to quantify bacterial cells in a label-free, inexpensive, and simple fashion.

9.3.2.1 Methods and device

9.3.2.1.1 Device

The device for electrical impedance measurements consists of a silica or glass chip patterned with an array of interdigitated microelectrodes (IMEs) and a microchamber (~25 μL capacity) right above the electrode area formed by silicone rubber, as shown in Figure 9.7(a). The interdigitated microelectrodes were fabricated on a flat silica or glass sub-

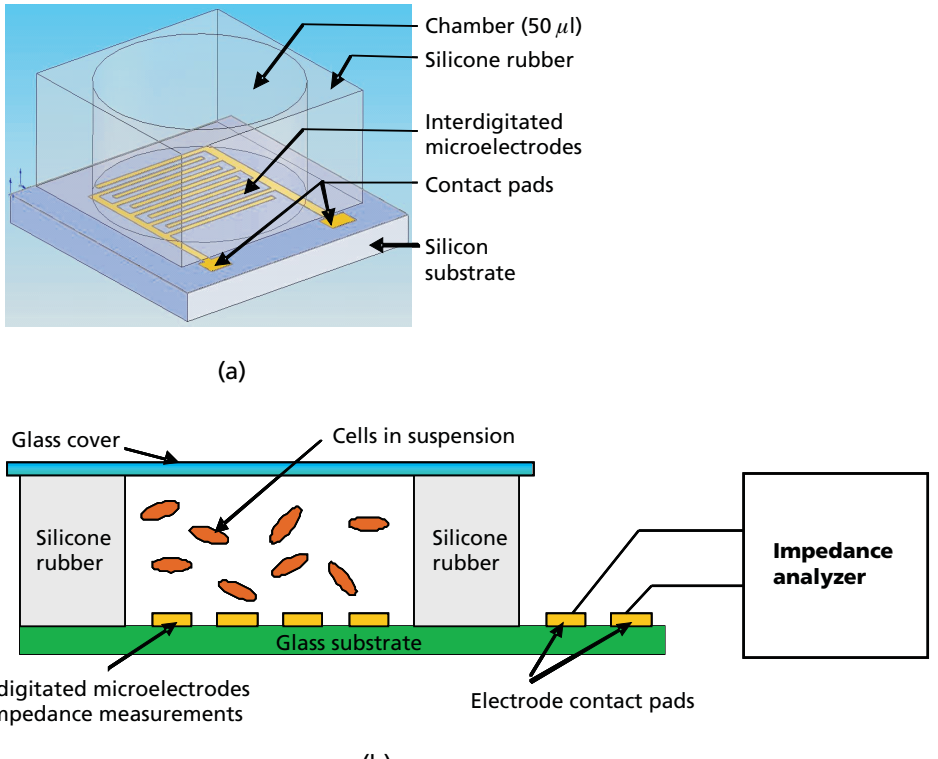

Figure 9.7 (a) The device for impedance detection of bacterial cells based on ion release from cells into buffers. It consists of a chamber formed by silicone rubber and a set of interdigitated microelectrodes at the floor of the chamber. The chamber capacity is 25 μL. The gold interdigitated microelectrode consists of 50 pairs of finger electrodes with 15 μm of digit electrode width and 15 μm interdigit space. (b) Schematic setup for electrical impedance spectroscopic measurements of impedance of bacterial cell suspensions in DI water or PBS. (Reprinted with permission from *Talanta* and kind permission from [1].)

strate using standard lithographic microfabrication technology. The IME consists of a pair of microband arrays of digit electrodes that mesh with each other. The width of digit electrodes and the interdigit space can be in the range of microns to nanometers, with a total of tens to hundreds of pairs of finger electrodes. The two sets of microelectrodes are used as the two poles in a bipolar impedance-measurement setup. The IMEs used in this experiment have a total of 50 pairs of finger electrodes with each having a width of 15 μm and a space of 15 μm. IMEs are also commercially available.

The chamber was made by punching a hole in a piece of silicon rubber using a standard puncher of a desired size. The silicon rubber was then glued to the chip using epoxy with the chamber appropriately aligned with the electrode area.

9.3.2.1.2 Preparation of bacteria cells

Stock culture of *Salmonella typhimurium* was purchased from Carolina Biological Supply Company (Burlington, North Carolina). The culture was grown in brain-heart-infusion (BHI) broth (TEKnova, Hollister, California) at 37°C for 16 to 18 hours. The cells were centrifuged (Eppendorf, Westbury, New York) at 6,000 × g for 2 minutes. After removal of the supernatant, the cell pellet was resuspended in sterilized DI water or PBS. The cells were washed three times with DI water or PBS in order to get rid of residues from the growth medium. Then, they were serially (1:10) diluted with DI water or PBS to desirable concentrations for further experiments.

The traditional plating method was used to determine the viable cell number in the stock cell suspension prepared in the above step. The cells suspension was serially (1:10) diluted with DI water. Then, 100 μL of appropriate dilutions were plated onto XLT4 agar plates (Difco, Sparks, Maryland). Colonies were counted after incubation of the plates at 37°C for 24 hours. Generally, the cell numbers in the stock cell suspension averaged about 10^9 cfu/mL.

9.3.2.1.3 Electrical impedance spectroscopy (EIS)

Impedance measurements were performed using an IM-6 impedance analyzer (Zahner-Elektrik Gmbh & CoKG, Kronach, Germany) with the IM-6/THALES software. Figure 9.7(b) shows the schematic impedance-measurement setup. For impedance measurements, 20 μL of each sample was placed into the microchamber and covered with a glass cover. One of the two microband array electrodes was connected to the test and sensing probes, and the other was connected to the reference and counter electrodes on the IM-6 impedance analyzer. EIS measurements were carried out in a frequency range from 1 Hz to 100 kHz. Bode (impedance and phase versus frequency) diagrams were recorded. Impedance at a fixed frequency was measured using the capacitance-potential (C/E) program at 1 kHz with an amplitude of ±50 mV. Impedance data were recorded at every minute. All tests were performed at room temperature.

Simulation was performed using the SIM program. From each measured spectrum, 50 data points were automatically selected by the software as the input, and the fitting curves were generated using an equivalent circuit model.

9.3.2.2 Results and discussion

9.3.2.2.1 Impedance spectra of bacterial cell suspensions in DI water and PBS

Figure 9.8 presents the Bode impedance spectra of *Salmonella typhimurium* cell suspensions in (a) DI water and (b) PBS, along with their equivalent circuits and best-fitting

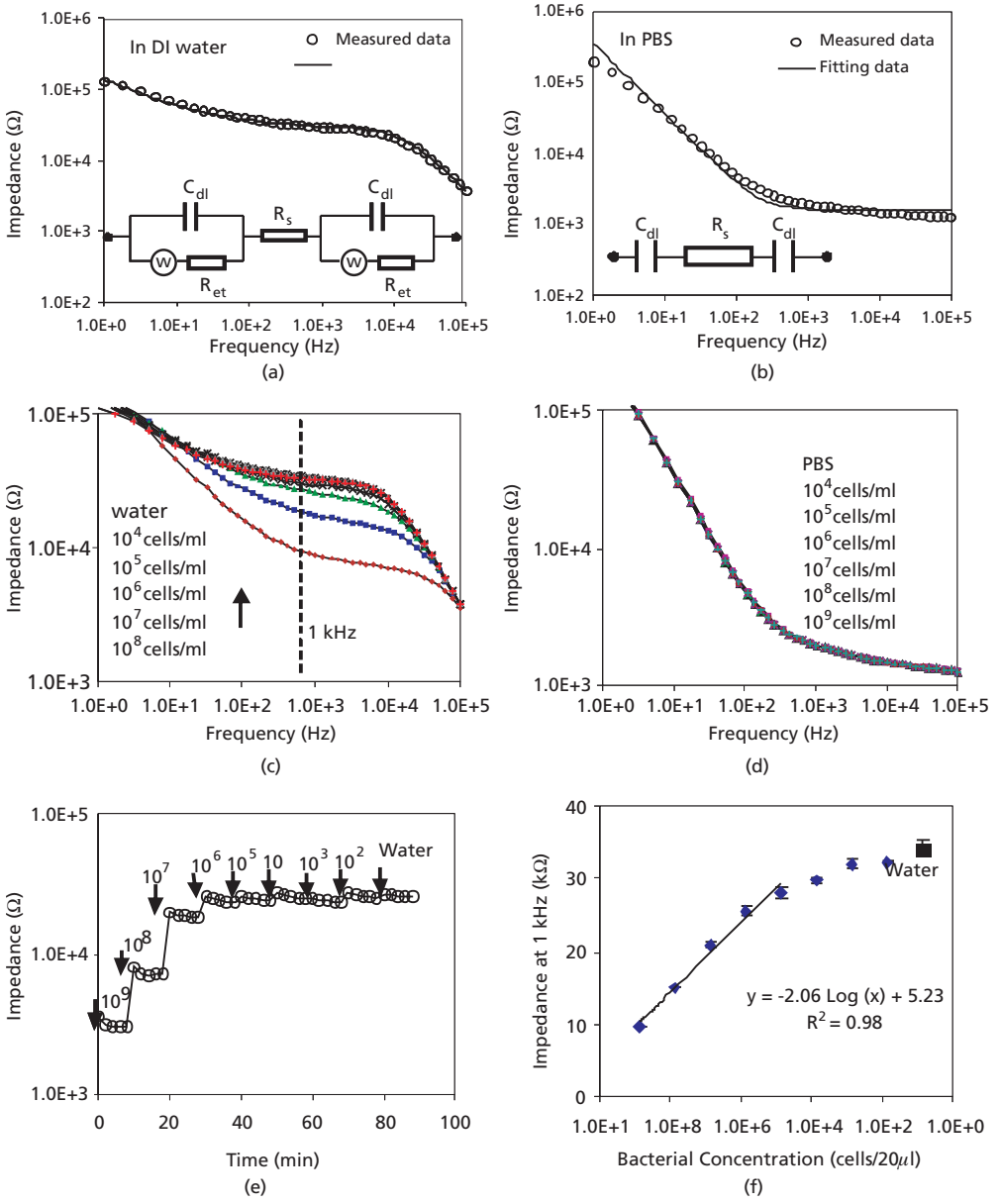

Figure 9.8 (a, b) Impedance spectra of *Salmonella* cell suspensions in (a) DI water and (b) PBS, together with their fitting curves and the equivalent circuits. *Salmonella* concentration: 1.93×10^6 cfu/mL. (c, d) Impedance spectra of *Salmonella* suspensions in (c) DI water and (d) PBS, with the cell concentrations in the range of 10^4 to 10^9 cfu/mL, along with samples of water and PBS as controls. (e) Typical impedance responses to the samples with different concentrations of cells when they were measured at a fixed frequency of 1 kHz. (f) The linear relationship between the logarithmic value of the concentration of *Salmonella* cells and the impedance measured at 1 kHz. Error bars are standard deviations of three to five measurements. Impedance spectra were measured in the frequency range of 1 Hz to 100 kHz with an amplitude of ±50 mV. (Reprinted with permission from *Talanta* and kind permission from [1].)

spectra. For *Salmonella* cell suspension in DI water, the measured spectrum [Figure 9.8(a), blank dots] is a typical Bode plot for a system in which the polarization is due to a combination of kinetic and diffusion processes. Based on the general electrical-equivalent model of an electrochemical cell [44] and the behavior of the IME microelectrode [45], the measured spectrum can be modeled by an equivalent circuit that consists of the ohmic resistance (R_s) of the solution between two electrodes, double-layer capacitance (C_{dl}), electron-transfer resistance (R_{et}), and Warburg impedance (Z_w) around each electrode. The agreement between the measured data and the fitting spectra (solid line) indicated that the equivalent circuits provided a feasible, if not unique, model to describe the impedance characteristics of *Salmonella* suspensions in DI water. Using this circuit model, the simulated values of C_{dl}, Z_w, R_{et}, and R_s were 884.9 pF, 147.2 kΩ/s$^{0.5}$, 13.54 kΩ, and 491.2Ω, respectively, with the mean error of modulus impedance of 0.6%. The spectrum and the circuit model suggest that electrochemical reactions occur on the IME electrodes and that the cells may have released some electrochemical active composites to the DI water.

For *Salmonella* suspensions in PBS, the impedance spectrum [Figure 9.8(b), blank dots] shows two domains: a double-layer region in the low-frequency range from 1 Hz to approximately 500 Hz, and a resistive region in the frequency range from approximately 500 Hz to 100 kHz. The electrical impedance behavior of the cell suspension in PBS can be represented by the equivalent circuit of the IME system in aqueous solutions reported previously [45–47]. In this circuit model, two identical double-layer capacitances (C_{dl}) of each set of the IME are connected to the medium resistance (R_s) in series. C_{dl} dominates the impedance in the low-frequency range (double-layer region), whereas R_s dominates the impedance in the high-frequency range (resistive region). By simulation, the values of C_{dl} and R_s were 892.8 nF and 1.62 kΩ, respectively, with the mean error of modulus impedance of 3.0%. In the cell suspension in PBS, the impedance spectrum does not show any characteristics related to electrochemical active parameters, which implies cells may not release active electrochemical species into PBS.

Figure 9.8(c, d) shows the Bode impedance spectra of *Salmonella* suspensions in (c) DI water and (d) PBS solution with different cell concentrations from 10^4 to 10^9 cfu/mL. It is observed that the suspensions with different cell concentrations in DI water each have a distinct impedance response in the frequency range from 100 Hz to 10 kHz, whereas impedance spectra of *Salmonella* suspensions in PBS were identical in the full frequency range. The results verified that when bacterial cells were suspended in low-conductive DI water, they could alter the conductivity of the suspension.

9.3.2.2.2 Quantifying bacterial concentration in DI water by impedance

As the solution impedance decreases with the increasing cell concentration in DI water within a certain frequency range, we can estimate the cell concentration in DI water using the impedance value at a fixed frequency. As the best representative frequency, 1 kHz was used to investigate the relationship between impedance values and cell concentrations in DI water suspensions. Figure 9.8(e) shows typical impedance responses at 1 kHz to samples of different bacterial concentrations. When the bacterial concentration decreased from 10^9 cfu/mL to 10^8, 10^7, and 10^6 cfu/mL, impedance of the suspensions significantly increased from 3.13 ± 0.26 kΩ to 7.29 ± 0.17, 18.7 ± 0.28, and 24.4 ± 0.58 kΩ. Figure 9.8(f) shows the plot of the impedance values as a function of the bacterial concentrations. There is a linear relationship between the impedance and the loga-

Troubleshooting Table

Problem	Explanation	Potential Solution
There is fluid leakage	The chip is not well assembled	Use a new and well assembled chip.
DEP does not capture cells or spores	The connection between the DEP electrodes and the DEP signal generator does not work	Check the connection or change to a new chip.
There is no signal in impedance measurements	There is a bad connection between the chip and the impedance instrument	Check the connections.
Impedance baseline with deionized water is not consistent when a different vial of water is injected into the device	Deionized water changes its conductance after it exposes to air	Prepare multiple vials of water in prerinsed clean tubes and sterilize the batch together. Discard any water vials that have been left open for more than 30 minutes.
Impedance baseline with deionized water from the same vial is not consistent	Impedance is affected by ion release from the polymer material for chip fabrication	Soak the whole chip in deionized water over night, or flush the channels with deionized water for an extended period (hours) until the baseline stabilizes with continuous injection of deionized water.
Cells don't lyse or lyse too quickly using the present lysis solution	Different cells have different tolerances for the hypotonic environment	For each cell type, the lysis solution needs to be optimized such that during the solution exchange from isotonic to hypotonic solution, the cells remain intact but will lyse rapidly after the lysis solution flow stops.
Impedance does not change after the germinant is injected	Spores germinate before reaching the detection chamber	One-time use of the device will prevent germination due to chemical residues. A separate inlet for germinant delivery is also recommended to avoid pregermination.

rithmic value of the cell concentration in the range from 10^4 to 10^8 cells/20 μL (10^6 to 10^{10} cfu/mL). The linear regression equation is Z (kΩ) = –2.06 Log C (cells/20 μL) + 5.23 with $R^2 = 0.98$. The detection limit was calculated to be 6.9×10^4 cells/20 μL (3.45×10^6 cfu/mL).

In this section, we have demonstrated a new, simple, and rapid method to detect bacterial cells by measuring the impedance properties of their suspensions in DI water using interdigitated microelectrodes. This method does not require any label or amplification steps. It can be used as an alternative approach to quantify bacterial cells in suspensions to impedance microbiology. The detection limit of this method is comparable with many other label-free immunosensors for detection of pathogenic bacteria using different transducer techniques, including QCM immunosensors for detection of *Salmonella* with detection limits of 3.2×10^6 cfu/mL and 9.9×10^5 cfu/mL [48, 49], SPR immunosensors for the detection of *Salmonella enteritidis* and *Listeria monocytogens* with detection limits of 10^6 cfu/mL [50], a SPR sensor for detection of *E. coli* O157:H7 with a detection limit of 10^7 cfu/mL [51], and an electrochemical impedance immunosensor for the detection of *E. coli* O157:H7 with a detection limit of 10^6 cfu/mL [10]. To afford this method with selectivity, we have recently implemented magnetic separation prior to the impedance detection [1]. To further improve the detection limit of this approach, a concentration step that enriches the small number of bacterial cells into a microdetection chamber would be very useful.

9.4 Conclusion

Advances in microfabrication have paved the way for miniaturization of many traditional detection platforms into microdevices or chips. Impedance sensing as a principal

electrical transducer technique is one of the best-suited measurement approaches that can be incorporated into microchips. We have demonstrated four microchip-based systems that have been successfully used for monitoring microbial and cellular activities and for detecting bacterial and mammalian cells. The microscale impedance-based methods have shown advantages in improved sensitivity, reduced quantities of costly reagents, reduced detection time, and flexibility in integration with other electrical methods such as DEP.

9.5 Summary Points

- The microfabricated systems described here demonstrate the application of microscale lab-on-a-chip devices for the detection of biological activities with high sensitivity and shortened assay time.
- Microscale "impedance microbiology" can be realized in a microchip format, which can be integrated with an electrical concentration step, through dielectrophoresis (DEP), for rapid detection of bacterial cells based on their metabolic activity.
- The DEP concentration in microchip "impedance microbiology" eliminates the traditional cell-growth-enrichment step and thus can significantly save assay time, which is a great improvement compared with conventional methods that require several days.
- Automatic and rapid electrical detection of the germination of viable spores can be achieved. DEP concentration of a low number of spores in the ultrasmall detection chamber (0.1 nL) within the microfluidic biochip can improve the detection limit down to fewer than 100 spores and significantly reduce the detection time compared with traditional methods.
- Microfluidic chip-based impedance spectroscopy can be designed to detect both mammalian and bacterial cells by monitoring the impedance change in the culture buffer as a result of ion release from the cells. The microdevice helps to confine the ions in a small volume for sensitive impedance measurement.

Acknowledgments

L. Yang acknowledges the funding from the Golden LEAF Foundation and the state of North Carolina through the Biomanufacturing Research Institute & Technology Enterprise (BRITE) Center for Excellence. X. Cheng and R. Bashir acknowledge support from the NIH/National Institute of Biomedical Imaging and Bioengineering under Grant No. P41 EB002503 (BioMEMS Resource Center, PI: Professor M. Toner). R. Bashir acknowledges research support through the Center for Food Safety Engineering at Purdue University, funded through a cooperative agreement with the Agricultural Research Service of the U.S. Department of Agriculture, project number 1935-42000-035. The authors also thank the staff and facilities of the Birck Nanotechnology Center at Purdue University.

References

[1] Yang, L., "Electrical impedance spectroscopy for detection of bacterial cells in suspensions using interdigitated microelectrodes," *Talanta*, Vol. 74, 2008, pp. 1621–1629.

[2] Pethig, R., and Markx, G. H., "Application of dielectrophresis in biotechnology," *TIBTECH*, Vol. 15, 1997, pp. 426–432.

[3] Silley, P., and Forsythe, S., "Impedance microbiology—a rapid change for microbiologists," *J. Applied Bacteriology*, Vol. 80, 1996, pp. 233–243.

[4] Wawerla, M., et al. "Impedance microbiology: Applications in food hygiene," *J. Food Protection*, Vol. 62, 1999, pp. 1488–1496.

[5] Gomez, R., Morisette, D. T., and Bashir, R., "Impedance microbiology-on-a-chip: Microfluidic bioprocessor for rapid detection of bacterial metabolism," *J. Microelectromechanical Systems*, Vol. 14, 2005, pp. 829–838.

[6] Liu, Y.-S., et al., "Electrical detection of germination of model *Bacillus anthracis* spores in microfluidic biochips," *Lab on a Chip*, Vol. 7, 2007, pp. 603–610.

[7] Cheng, X., et al., "Cell detection and counting through cell lysate impedance spectroscopy in microfluidic devices," *Lab on a Chip*, Vol. 7, No. 6, 2007, pp. 746–755.

[8] Giaever, I., and Keese, C. R., "Micromotion of mammalian cells measured electrically," *Proc. Natl. Acad. Sci. USA*, Vol. 88, 1991, pp. 7896–7900.

[9] Giaever, I., and Keese, C. R., "A morphological biosensor for mammalian cells," *Nature*, Vol. 366, 1993, pp. 591–592.

[10] Yang, L., Li, Y., and Erf, G. F., "Interdigitated array microelectrode-based electrochemical impedance immunosensor for detection of *Escherichia coli* O157:H7," *Analytical Chemistry*, Vol. 76, 2004, pp. 1107–1113.

[11] Gibson, D. M., Coombs, P., and Pimbley, D. W., "Automated conductance method for the detection of salmonella in foods—collaborative study," *J. AOAC International*, Vol. 75, 1992, pp. 293–302.

[12] AOAC, "Salmonella in food, automated conductance methods: AOAC official method 991.38," *Official Methods of Analysis of AOAC International*, 16th ed., Gaithersburg, MD: Association of Official Analytical Chemists International, 1996.

[13] Owicki, J., and Parce, J., "Biosensors based on the energy metabolism of living cells: The physical chemistry and cell biology of extracellular acidification," *Biosensors and Bioelectronics*, Vol. 7, 1992, pp. 257–272.

[14] Gomez, R., Bashir, R., and Bhunia, A., "Microscale electronic detection of bacterial metabolism," *Sens. Actuators B: Chemical*, Vol. 86, 2002, pp. 198–208.

[15] Gomez, R., et al., "Microfluidic biochip for impedance spectroscopy of biological species," *Biomedical Microdevices,* Vol. 3, 2001, pp. 201–209.

[16] Pohl, H. A., *Dielectrophoresis*, Cambridge, U.K.: Cambridge University Press, 1978.

[17] Jernigan, J. A., et al., "Bioterrorism-related inhalation anthrax: The first 10 cases reported in the United States," *Emerging Infectious Diseases*, Vol. 7, No. 6, 2001, pp. 933–944.

[18] Straiger, P., and Losick, R., "Molecular genetics of sporulation in bacillus subtilis," *Annual Review of Genetics*, Vol. 30, 1996, pp. 297–341.

[19] Nicholson, W. L., et al., "Resistance of bacillus endospores to extreme terrestrial and extraterrestrial environments," *Microbiology and Molecular Biology Reviews*, Vol. 64, 2000, pp. 548–572.

[20] Hartley, H. A., and Baeumner, A. J., "Biosensor for the specific detection of a single viable *B. anthracis* spore," *Analytical and Bioanalytical Chemistry*, Vol. 376, No. 3, 2003, pp. 319–327.

[21] Ryu, C., et al., "Sensitive and rapid quantitative detection of anthrax spores isolated from soil samples by real-time PCR," *Microbiology and Immunology*, Vol. 47, 2003, pp. 693–699.

[22] Lee, J., and Deininger, R. A., "A rapid screening method for the detection of viable spores in powder using bioluminescence," *Luminescence*, Vol. 19, 2004, pp. 209–211.

[23] Welkos, S. L., et al., "A microtiter fluorometric assay to detect the germination of *Bacillus anthracis* spores and the germination inhibitory effects of antibodies," *J. Microbiological Methods*, Vol. 56, 2004, pp. 253–265.

[24] Hamouda, T., Shih, A. Y., and Baker, J. R., Jr., "A rapid staining technique for the detection of the initiation of germination of bacterial spores," *Letters in Applied Microbiology*, Vol. 34, No. 2, 2002, pp. 86–90.

[25] Kiel, J. L., et al., "Growth medium for the rapid isolation and identification of anthrax," *Proc. SPIE*, Vol. 4036, 2000, pp. 92–102.

[26] Hindson, B., et al., "APDS: The autonomous pathogen detection system," *Biosensors and Bioelectronics*, Vol. 20, 2005, pp. 1925–1931.

[27] Titball, R. W., and Manchee, R. J., "Factors affecting the germination of spores of *Bacillus anthracis*," *J. Applied Bacteriology*, Vol. 62, 1987, pp. 269–273.

[28] Chang, W. J., et al., "Hybrid poly(dimethylsiloxane) (PDMS)/silicon biochips for bacterial culture applications," *Biomedical Microdevices*, Vol. 5, 2003, pp. 281–290.

[29] Agirregabiria, M., et al., "Fabrication of SU-8 multilayer microstructures based on successive CMOS compatible adhesive bonding and releasing steps," *Lab on a Chip*, Vol. 5, 2005, pp. 545–552.

[30] Baek, J. Y., et al., "A pneumatically controllable flexible and polymeric microfluidic valve fabricated via in situ development," *J. Micromech. Microeng.*, Vol. 15, 2005, pp. 1015–1020.

[31] Yang, L., et al., "A multifunctional microfluidic system for dielectrophoretic concentration coupled with immuno-capture of low number of *Listeria* monocytogenes," *Lab on a Chip*, Vol. 6, 2006, pp. 896–905.

[32] Gawad, S., Schild, L., and Renaud, P., "Micromachined impedance spectroscopy flow cytometer for cell analysis and particle sizing," *Lab on a Chip*, Vol. 1, 2001, pp. 76–82.

[33] Kruger, J., et al., "Development of a microfluidic device for fluorescence activated cell sorting," *J. Micromech. Microeng.*, Vol. 12, No. 4, 2002, pp. 486–494.

[34] Huh, D., et al., "Use of air-liquid two-phase flow in hydrophobic microfluidic channels for disposable flow cytometers," *Biomedical Microdevices*, Vol. 4, No. 2, 2002, pp. 141–149.

[35] Koch, M., Evans, A. G. R., and Brunnschweiler, A., "Design and fabrication of a micromachined coulter counter," *J. Micromech. Microeng.*, Vol. 9, No. 2, 1999, pp. 159–161.

[36] Lundien, M. C., et al., "Induction of MCP-1 expression in airway epithelial cells: Role of CCR2 receptor in airway epithelial injury," *J. Clin. Immunol.*, Vol. 22, No. 3, 2002, pp. 144–152.

[37] Giaever, I., and Keese, C. R., "Monitoring fibroblast behavior in tissue-culture with an applied electric-field," *Proc. Natl. Acad. Sci. USA*, Vol. 81, No. 12, 1984, pp. 3761–3764.

[38] Ehret, R., et al., "Monitoring of cellular behaviour by impedance measurements on interdigitated electrode structures," *Biosensors and Bioelectronics*, Vol. 12, No. 1, 1997, pp. 29–41.

[39] Van Der Wal, A., et al., "Conductivity and dielectrical dispersion of gram-positive bacterial cells," *J. Colloid Interface Sciences*, Vol. 186, 1997, pp. 71–79.

[40] Wilson, W. W., et al., "Status of methods for assessing bacterial cell surface charge properties based on zeta potential measurements," *J. Microbiological Methods*, Vol. 43, 2001, pp. 153–164.

[41] Carstensen, E. L., and Marquis, R. E., "Passive electrical properties of microorganisms. III. Conductivity of isolated bacterial cell walls," *Biophys. J.*, Vol. 8, 1968, pp. 536–548.

[42] Mozes, N., and Rouxhet, P. G., "Microbial hydrophobicity and fermentation technology," in R. J. Doyle and M. Rosenberg, (eds.), *Microbial Cell Surface Hydrophobicity*, Washington, D.C.: American Society for Microbiology, 1990, pp. 75–105.

[43] Baldwin, W. W., et al., "Changes in buoyant density and cell size of *Escherichia coli* in response to osmotic shocks," *J. Bacteriology*, Vol. 170, No 1, 1988, pp. 452–455.

[44] Bard, A. J., and Faulkner, L. R., *Electrochemical Methods: Fundamentals and Applications*, New York: John Wiley & Sons, 2001.

[45] Van Gerwen, P., et al., "Nanoscaled interdigitated electrode arrays for biochemical sensors," *Sens. Actuators B: Chemical*, Vol. 49, 1998, pp. 73–80.

[46] Laureyn, W., et al., "Nanoscaled interdigitated titanium electrodes for impedimetric biosensing," *Sens. Actuators B: Chemical*, Vol. 68, 2000, pp. 360–370.

[47] Yang, L., et al., "Interdigitated microelectrode (IME) impedance sensor for the detection of viable salmonella typhimurium," *Biosensors and Bioelectronics*, Vol. 19, 2004, pp. 1139–1147.

[48] Park, I., and Kim, N., "Thiolated salmonella antibody immobilization onto the gold surface of piezoelectric quartz crystal," *Biosensors and Bioelectronics*, Vol. 13, 1998, pp. 1091–1097.

[49] Park, I., Kim, W., and Kim, N., "Operational characteristics of an antibody-immobilized QCM system detecting salmonella spp," *Biosensors and Bioelectronics*, Vol. 15, 2000, pp. 167–172.

[50] Koubova, V., et al., "Detection of foodborne pathogens using surface plasmon resonance biosensors," *Sens. Actuators B: Chemical*, Vol. 74, 2001, pp. 100–105.

[51] Fratamico, P. M., et al., "Detection of *E. coli* O157:H7 using a surface-plasmon resonance biosensor," *Biotechnology Techniques*, Vol. 12, 1998, pp. 571–576.